



Utilization of Doped Nanoparticles of ZnO and TiO₂ as Antimicrobial Agent (A-Review)

**MAJED AL-SHAERI^{1,2}, RUKHSANA SATAR³, SYED ISMAIL AHMED⁴, MOHAMMED OVES⁵,
SHAKEEL AHMED ANSARI^{6,7} and SANDESH CHIBBER^{8*}**

¹Department of Biological Sciences, Faculty of Science, King Abdulaziz University, Jeddah, Saudi Arabia.

²Center of Excellence in Bionanoscience Research, King Abdulaziz University, Jeddah, Saudi Arabia.

³Department of Biochemistry, Ibn Sina National College for Medical Studies, Jeddah, Saudi Arabia.

⁴Physics Division, Department of Basic Sciences, Ibn Sina National College for Medical Studies, Jeddah, Saudi Arabia.

⁵Center of Excellence in Environmental Studies, King Abdulaziz University, Jeddah, Saudi Arabia.

⁶Center of Excellence in Genomic Medicine Research, King Abdulaziz University, Jeddah, Saudi Arabia.

⁷Department of Medical Laboratory Technology, Faculty of Applied Medical Sciences, King Abdulaziz University, Jeddah, Saudi Arabia.

⁸Division of Biological and Life Sciences, School of Arts and Sciences, Ahmedabad University, Ahmedabad, India.

*Corresponding author E-mail: sandesh.chibber@ils.ahduni.edu.in

<http://dx.doi.org/10.13005/ojc/350346>

(Received: June 03, 2019; Accepted: June 17, 2019)

ABSTRACT

Nanotechnology deals with the measurement and modeling of matter at nanoscale level by integrating the field of engineering and technology. Nanoparticles (NPs) have to be characterized for chemical, physical, optical and electrical properties followed by their catalytic assessment for exploiting their potential in antimicrobial aspects. Recent interest in nanotechnology witnessed the importance of doped NPs in various biomedical fields. Some of the prominent features of doped NPs that imparts them greater antimicrobial activity involves their stabilization, large surface area to volume ratio, and their ability to generate reactive oxygen species as a result of modification of band structure by introducing dopants into them. The types of dopants, synthesis techniques and experimental parameters are known to affect the overall electronic structure of the material, which leads to varied antibacterial efficiency. This review article provides in-depth information of utilization of doped nanoparticles of ZnO and TiO₂ which are actively in pursuit for antibacterial potential against various bacterial and fungal strains.

Keywords: Antimicrobial potential, Doped nanoparticles, ZnO, TiO₂, Reactive oxygen species.



INTRODUCTION

Nanotechnology involves the designing and formulation of matter at nanometer scale from their bulk counterparts by incorporating the field of engineering and technology¹. One of the important feature that attracts the use of these engineered materials included their manipulation and modification for generating novel functional properties². This approach is increasingly exploited on diverse products such as foods, testing kits, sensors in security systems, in health and medical products^{3,4}.

Nanotechnology based approaches are more exciting and hence exploited for preparing antimicrobial systems for biomedical applications by reducing or killing the activity of numerous microorganisms⁵. Researchers have observed that titanium and zinc exhibit greater antimicrobial potential when reoriented to nanoscale due to their potential of generating reactive oxygen species and offered increased surface area⁶. The effectiveness against bacteria owe to many favorable attributes of NPs such as their size and physical nature, their interaction with microorganisms, and their great potential in penetrating the bacterial cell⁷. However, NPs based antimicrobial systems suffer from limitations owing largely due to overwhelming growth and reproduction of bacteria and their capability of developing resistance against various bacterial population⁸⁻¹¹.

Zinc oxide nanoparticles (ZnO-NPs) represents an important metal oxide NPs owing to their peculiar physical and chemical properties. They are being employed in rubber industry as they can provide wear-proof of the rubber composite, improve performance of high polymer in their toughness and intensity, and antiaging. Due to the strong UV absorption property of ZnO, it is increasingly used in personal care products such as cosmetics and sunscreen. In addition, ZnO-NPs have superior antibacterial, antimicrobial and excellent UV-blocking properties. Therefore in the textile industry, the fabrics finished by adding ZnO-NPs exhibited the attractive functions of UV and visible light resistance, antibacterial and deodorant. Their utility is extended in other fields like concrete production, photocatalysis, electronics and electro-technology industries¹².

Titanium dioxide (TiO₂) is found in various consumer goods and products of daily use such

as cosmetics, paints, dyes and varnishes, textiles, paper and plastics, food and drugs. Due to its high diffraction index, and strong light scattering and incident-light reflection capability, TiO₂ is mostly used as white pigment. Moreover, its strong UV resistance makes TiO₂ the standard pigment found in white dispersion paints. Currently, they are mainly found in high-factor sun protection creams, textile fibers or wood preservatives. The better dispersion properties and photostability of TiO₂ are achieved by coating with other materials. TiO₂-NPs exists in two phases, rutile and anatase. While the rutile TiO₂ are applied mainly in suncreams, paints and dyes, the anatase TiO₂ are rather suited for photocatalysis. In the presence of UV radiation, anatase TiO₂ can form radicals from air or water which can degrade oxidatively organic pollutants. Due to their hydrophilic character, water forms a closed film on the surface in which pollutants, degradation products and microbial agents can be easily carried away¹³.

Importance of doped NPs as antimicrobial agents

Due to the occurrence of several biological processes at nanoscale level, it is quite possible that engineered nanomaterials may play significant role in such cellular processes. The modification of surface properties of metal oxide NPs as a result of doping with special atom(s) improved the optical and electrical properties of these NPs. Metal oxide NPs can be deposited on bacteria's surface or can be accumulated in the periplasmic region and for disrupting the cellular function for disorganizing the membranes. Doped NPs are favorable largely as they offer improved interaction to bacterial surfaces for ensuring better antibacterial effects^{14,15}. The possible mechanism might be that doped NPs interacts with the nucleic acid and protein for promoting deformation and structural changes in the DNA, protein and some growth factor which ultimately leads to change in metabolic pathway¹⁶⁻¹⁸. The presence of dopant to NPs may result in generation of higher amount of ROS that is required for disrupting the membrane structure which leads to bacterial death. Mechanistically, these NPs bind membrane lipids and liberates ROS to release free radicals with significantly enhanced antibacterial action Fig.1. Moreover, doped NPs can be coated on to surfaces for better use of their antimicrobial action as they exhibit greater stability in aqueous dispersion for longer durations.

Antimicrobial efficacy of doped ZnO-NPs

Zinc oxide is listed as GRAS for its antibacterial activity by Food and Drug Administration,

USA. Hence, it is extensively used to prepare food cans for packaging corn, meat, fish and peas for preserving colors and preventing spoilage. ZnO-NPs exhibited small size and high surface area which allowed them to interact with bacteria. Such properties imparts enhanced antimicrobial potential to these NPs as compared to their bulk counterpart. Recent studies suggested their toxicity to selective bacteria with minimal effects to human cells thereby making them highly suitable for designing antimicrobial probes¹⁹. Many studies on ZnO-NPs exhibited wide range of antibacterial activities^{20,21}.

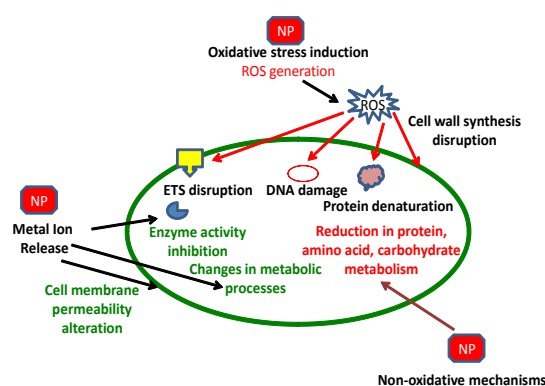


Fig. 1. Antibacterial action mechanism of doped nanoparticles

Table 1: Dopants used to increase the antimicrobial potential of ZnO-NPs

S. no.	Dopant	Microbial organisms	Antimicrobial activity	Reference
1	Cobalt and Iron	<i>S. aureus</i> , <i>B. cereus</i> , <i>S. typhi</i> , <i>E. coli</i>	Antibacterial efficacy against these strains by MIC method showed that co-doped ZCF10 and ZCF5 nanoparticles exhibited 40-50% increase in ZOI as compared to pure ZF.	22
2	Copper	<i>E. coli</i> , <i>E. coli</i> ,	The bactericidal property was found to be concentration dependent and ZnO-NPs with 5% Cu dopants show the maximum inhibition against bacterial growth. ZOI obtained for <i>K. pneumoniae</i> and <i>E. coli</i> by ZnO-NPs was 9 mm and 10 mm, respectively while these values were 11 mm and 14 mm for Nd doped ZnO-NPs.	23 24
3	Neodymium	<i>K. pneumonia</i> <i>S. mutans</i> , <i>P. aeruginosa</i>	ZOI observed by undoped and doped NPs was 10 mm and 20 mm, respectively for <i>S. mutans</i> . However, these values were 12 mm and 23 mm, respectively, for <i>P. aeruginosa</i> .	33
4	Nickel	<i>S. dysenteriae</i> , <i>V. cholerae</i> , <i>E. coli</i>	Antibacterial activity observed by Ni doped ZnO-NPs was 30%, 25% and 23% against <i>S. dysenteriae</i> , <i>V. cholerae</i> and <i>E. coli</i> , respectively, as compared to 16%, 7% and 5%, respectively, against these bacterial strains for undoped (pure) ZnO-NPs.	25
5	Fluorine	<i>E. coli</i> , <i>S. aureus</i>	The number of organisms grown in the presence of pure ZnO-NPs decreased with time for the first 3 h and then remained same. However, enhanced antimicrobial activity was observed when the organism was grown in the presence of F-doped ZnO-NPs under visible light.	26
6	Aluminium	<i>S. aureus</i> , <i>P. aeruginosa</i> , <i>S. typhimurium</i> , <i>K. pneumonia</i>	ZOI for Al doped ZnO-NPs was enhanced by 30-50% as compared to pure ZnO-NPs against various bacterial strains.	27
7	Tantalum	<i>B. subtilis</i> , <i>S. aureus</i> , <i>E. coli</i> ,	For <i>E. coli</i> and <i>S. aureus</i> , no significant antibacterial activity was observed for pure ZnO. The lowest MIC for <i>E. coli</i> , <i>S. aureus</i> and <i>B. subtilis</i> was 180, 200, and 160 µg/ml after adding the 5% Ta-doped nanoparticles into the tubes, respectively.	28
8	Manganese	<i>P. aeruginosa</i> , <i>E. coli</i> , <i>B. subtilis</i>	ZOI of ZnS:Mn ²⁺ nanoparticles against <i>E. coli</i> and <i>B. subtilis</i> was 32 mm and 35 mm as compared to 15 and 20 mm ZOI, respectively by undoped ZnS.	29
9	Plant extract	<i>E. coli</i> , <i>S. typhi</i> , <i>P. aeruginosa</i>	ZOI value for <i>E. coli</i> at 40 mg concentration was 13 mm and 15 mm when red and white flower extracts were used as dopants, respectively. However these values were 15 mm and 20 mm, and 15 mm and 17 mm for <i>S. typhi</i> and <i>P. aeruginosa</i> , respectively under identical experimental conditions.	31
10	Cobalt	<i>E. coli</i> , <i>V. cholerae</i>	ZOI of pure ZnO-NPs was 13 mm, 15 mm, 17 mm and 18 mm for <i>S. dysenteriae</i> , <i>S. typhi</i> , <i>V. cholera</i> and <i>E. coli</i> , respectively while for 5% Co doped ZnO-NPs, these values were 17 mm, 20 mm, 21 mm and 22 mm, respectively.	32

11	Manganese and Iron	<i>S. aureus</i> , <i>E. coli</i> , <i>K. pneumoniae</i> , <i>S. typhi</i> , <i>C. albicans</i> , <i>A. fumigates</i> , <i>C. neoformans</i> , <i>T. mentegrophytes</i>	MIC for undoped ZnO was 0.16-0.43 mg/ml in case of bacteria. The most effective value of MIC was obtained against <i>S. typhi</i> and <i>E. coli</i> at 0.16 mg/ml while MIC observed for <i>T. mentegrophytes</i> and <i>C. neoformans</i> was 0.33 mg/ml and 26.6 mg/ml, respectively. Moreover, MIC of 0.09 mg/ml was obtained with 10% Fe doping for <i>B. subtilis</i> followed by 0.11 mg/ml for <i>E. coli</i> and 0.12 mg/ml for <i>S. aureus</i> at the same doping concentration. In case of 1% Fe doping, of all the pathogenic microbes used <i>S. typhi</i> showed best results at 0.13 mg/ml MIC. MIC values for both the fungal strains, i.e. <i>T. mentegrophytes</i> and <i>C. neoformans</i> were 0.25±0.21 mg/ml and <i>P. aeruginosa</i> , <i>B. subtilis</i> , 11.5±11.8 in case of 10% Fe doping and 0.33±0.14 mg/ml and 13.5±10.9 mg/ml in case of 1% Fe doping, respectively.	30
12	Yttrium	<i>E. coli</i> , <i>B. subtilis</i> , <i>S. typhi</i>	Pure ZnO-NPs showed maximum antibacterial activity against <i>S. aureus</i> , i.e., 18 mm as compared to 16 mm by 15% Y doped ZnO-NPs.	35
13	Cerium and Iron	<i>S. aureus</i> , <i>K pneumoniae</i> , <i>E. coli</i> , <i>P. aeruginosa</i> , <i>B. subtilis</i>	At 100 microlitre/well concentration of ZnO-NPs, ZOI (mm) was 9, 8, 12, 12 and 11 for <i>S. aureus</i> , <i>K. pneumoniae</i> , <i>E. coli</i> , <i>P. aeruginosa</i> and <i>B. subtilis</i> , respectively. However, these values were 24, 25, 24, 28 and 23 mm, respectively for the doped ZnO-NPs.	39
14	Silver and Nickel	<i>B. subtilis</i> , <i>P. aeruginosa</i>	The photocatalytic activity of ZnO-NPs was improved for decolorization efficiency of methyl violet (industrial pollutant) by Ag doping with optimum 2%. ZOI for ZnO-NPs and Ni-doped ZnO-NPs against <i>P. aeruginosa</i> and <i>B. subtilis</i> was 4-8 mm and 9-14 mm, respectively.	36 37
15	Copper oxide	<i>E. coli</i> , <i>S. aureus</i>	ZOI for prickly Zn-CuO-NPs were 24.2 and 26.8 mm for <i>E. coli</i> and <i>S. aureus</i> , respectively, while the corresponding data for Zn-CuO nanorods were 0 and 20.1 mm.	38

Table 2: Dopants used to increase the antimicrobial potential of TiO₂-NPs

S. no.	Dopant	Microbial organisms	Antibacterial activity	References
1	AgNPs	<i>S. aureus</i> , <i>P. aeruginosa</i> , <i>E. coli</i> , <i>S. epidermidis</i> ,	The viability of <i>S. aureus</i> , <i>P. aeruginosa</i> and <i>E. coli</i> was reduced to zero at 3% and 7% Ag-doped TiO ₂ -NPs. However, annealed TiO ₂ showed zero viability at 80 mg/30 mL where as doped Ag-TiO ₂ 7% showed zero viability at 40 mg/30 mL culture in the case of <i>P. aeruginosa</i> only. Undoped NPs does not show any antibacterial activity against <i>S. aureus</i> and <i>E. coli</i> . However, Ag doped and chitosan doped TiO ₂ -NPs exhibited excellent bacterial inhibition zone. The size and ZOI increases with the increase in Ag content. Interestingly, ZOI was more for Ag/chitosan capped TiO ₂ -NPs as compared <i>S. aureus</i> , <i>E. coli</i> to Ag doped TiO ₂ -NPs. The OD of bacterial culture media was reduced by 95% in the presence of Ag doped TiO ₂ -modified NRLF after 3 h as compared to 50% by TiO ₂ -modified NRLF under similar experimental conditions.	49 45 51
2	Cerium	<i>E. coli</i>	In 1 mg/ml cerium doped TiO ₂ -NPs, only 38 colonies were observed as compared to 120 colonies observed for pure TiO ₂ -NPs.	46
3	Iron and Indium	<i>E. coli</i> , <i>S. aureus</i>	A significant decrease was observed in <i>S. aureus</i> at 500 µg/ml concentration of 0.5% indium doped TiO ₂ -NPs.	47
4	SiO ₂	<i>P. aeruginosa</i> , <i>E. coli</i>	ZOI (mm) for pure and TiO ₂ -SiO ₂ -Ag nanocomposite obtained for <i>S. aureus</i> was 12 and 16, respectively; <i>K. pneumonia</i> was 14 and 18, respectively; <i>E. coli</i> was 14 and 17, respectively; <i>P. aeruginosa</i> was 15 and 21, respectively; <i>A. niger</i> was 11 and 14, respectively; Trichophyton was 14 and 20, respectively; Fusarium was 12 and 16, respectively; and Mucor was 12 and 16, respectively. Ag doped TiO ₂ -SiO ₂ catalyst showed superior photoactivity against <i>E. coli</i> as compared to the gel-derived TiO ₂ -SiO ₂ counterpart under similar experimental conditions.	50
5	Nitrogen	<i>S. pyogenes</i> , <i>E. coli</i> , <i>S. aureus</i> , <i>A. baumannii</i>	AgNPs impregnated N-doped titania films exhibited strong visible-light enhanced antibacterial properties and improved durability as compared to undoped NPs.	52

Since, the doping of NPs results in generation of higher amount of ROS which is needed for disrupting the cell for inducing bacterial death, researchers have earlier formulated Co/Fe doped and Co-Fe Co-doped ZnO-NPs (of composition $Zn_{0.85}Co_{0.15-x}Fe_xO$ where $x = 0, 0.15, 0.10, 0.05$ labeled as ZC, ZF, ZCF10, ZCF5) by mechanochemical method. XRD results suggested that Co/Fe doped and Co-Fe co-doped ZnO-NPs possess wurtzite crystal with hexagonal structure with an average crystallite size between 17-32 nm. FTIR result showed the presence of absorption bands in $478-445\text{ cm}^{-1}$ region due to $\nu Zn-O$ mode which indicated that Co and Fe have substituted Zn in ZnO matrix²². SEM images revealed that Co doped ZnO nanocrystalline powder (ZC) possesses spherical structure whereas Fe doped (ZF) and (Co, Fe) co-doped (ZCF10 and ZCF5) samples have shown hexagonal structures. The antimicrobial potential of the prepared samples were observed in *Gram positive* bacteria such as *B. cereus* and *S. aureus*, and in *Gram negative* bacteria including *S. typhi* and *E. coli*. MIC method has shown ZC, and co-doped ZCF10 and ZCF5 NPs constitute promising antibacterial agents as compared to ZF. In another approach, sol-gel technique was used to prepare $Zn_{1-x}Cu_xO$ ($x = 0.00, 0.01, 0.03, \text{ and } 0.05$) NPs by employing nitrate and gelatin as precursors. Further, the effect of various concentration of copper was observed on other bacterial strains. XRD result illustrated the doping of Cu into ZnO-NPs. Field emission SEM revealed their spherical shape which measures 30-52 nm. Doping with copper generated Cu-O-Zn structure on the surface which was responsible for decrease in its crystalline size and increase in the energy band gap. Moreover, it was observed that Cu doped ZnO-NPs show better antimicrobial potential against *E. coli* as observed by measuring the zone of inhibition (ZOI) diameter²³.

Neodymium (Nd) was earlier used to dope ZnO-NPs to improve its properties by co-precipitation technique. Zn-O stretching bands were observed at 422 and 451 cm^{-1} for ZnO-NPs and Nd doped ZnO-NPs, respectively as observed by FTIR spectroscopy. UV-Vis spectroscopy revealed the presence of excitonic peaks at 373 nm and 380 nm for the formulated samples. Antimicrobial screening of these nanomaterials against *E. coli* and *K. pneumoniae* exhibited that Nd doped ZnO-NPs were superior as compared to undoped ZnO-NPs. Moreover,

SEM showed negligible viability of bacterial cell because of impairment of cell membrane integrity²⁴. In another study, ZnO-NPs were doped with Ni to observe their antimicrobial effect against *V. cholera*, *S. dysenteriae* and *E. coli*. Ni-doped ZnO-NPs represents hexagonal wurtzite structure as revealed by XRD analysis. Additionally, the shifting of XRD peaks for the doped NPs gave clues for the Ni ions incorporated well in the ZnO lattice. SEM confirmed the formation of nanocrystallites with spherical shape. EDS spectroscopy indicated that Ni^{2+} was substituted in lattice site of Zn^{2+} . The optical property of the designed doped NPs was further substantiated by UV-Vis studies which indicated that Ni-doped ZnO-NPs enhanced the antibacterial potential in *E. coli* and *V. cholera* as compared to pure ZnO-NPs²⁵. *S. aureus* and *E. coli* when employed to evaluate the antimicrobial properties of F doped ZnO-NPs confirmed the same²⁶. It was further noticed that F-doping was more effective against *E. coli* and *S. aureus* as compared to pure ZnO-NPs after irradiated with visible light.

Doping of ZnO-NPs by aluminum had shown improved antibacterial activities against many bacterial strains like *S. aureus*, *P. aeruginosa*, *S. typhimurium* and *K. pneumoniae*²⁷. Moreover, ZnO-NPs were doped using Ta by Guo and coworkers, and their antimicrobial study was carried on *E. coli*, *S. aureus*, *P. aeruginosa* and *B. subtilis* by a standard microbial method²⁸. MIC results indicated that such Ta^{5+} ions incorporates into ZnO and improved their bacteriostasis effect on many strains under the absence of light. Alternately, doped ZnO-NPs showed high bactericidal efficacy in dark as witnessed by MIC results. Such improvement in antibiotic efficiency in dark conditions may be hypothesized due to combined effect of enhanced electrostatic force and surface bioactivity.

ZnS-NPs were doped with Mn^{2+} and modified by thio-glycolic acid to estimate its antimicrobial utility against *B. subtilis* and *E. coli*. It was observed that *B. subtilis* showed greater antimicrobial effect (35 mm) to Mn doped NPs at 50 mM. However, ZOI (20 mm) was maximum for *E. coli* under similar incubation conditions²⁹. Sharma *et al.*, (2016) have earlier developed the combination therapy of antibiotics and doped ZnO-NPs that can be used against MDR microorganisms³⁰. The doped ZnO-NPs showed enhanced antimicrobial potential as compared to pure ZnO-NPs.

Green nanotechnology was also attempted for pathogen detection and environmental protection [Shoba *et al.*, 2013]. These workers exploited ethanolic extract of *Bougainvillea glabra* as dopant to dope MgS-NPs and observed that they display promising antibacterial activity. Interestingly, it was observed that MgS-NPs doped with white colored flower extracts enhanced the antimicrobial potential significantly as compared to doping with red colored flower extracts. They hypothesized that white flowers may contain active antibacterial component and can be suggested as an antibiotic agent to inhibit the bacterial growth³¹. Cobalt doped ZnO-NPs exhibited greater effects against water borne bacteria. XRD and SEM results suggested the crystalline single phase structure. Doping of ZnO-NPs with Co, coupled with sunlight exposure further elevates the antimicrobial activity for water borne isolates of bacteria like *E. coli* and *V. cholerae*³².

An attempt was made to dope ZnO-NPs with trivalent neodymium (Nd^{3+}) to improve the optical and antibacterial performance against certain human pathogenic bacteria. The high resolution SEM images pointed to spindle shaped structure, and the presence of Nd^{3+} ions was indicated through EDS spectroscopy. Greater concentration of Nd^{3+} used to dope ZnO-NPs exhibited enhanced antimicrobial potential than the lower concentration of Nd^{3+} used for doping. This effect was due to the oxygen vacancies created that leads to the electron-hole pairs of the NPs³³. Sharma and coworkers have studied the antimicrobial activities of ZnO-NPs that were doped with Mn/Fe against *S. typhi*, *B. subtilis*, *S. aureus*, *E. coli*, *P. aeruginosa* and *K. pneumoniae*, and several fungi including *T. mentegrophytes*, *A. fumigatus*, *C. albicans* and *C. neoformans*. The formulated doped NPs were evaluated for their photocatalytic activities by degrading methylene blue dye in aqueous solution under UV light irradiation. It was observed that ZnO-NPs doped with 10% of Mn and Fe ions exhibited maximum antimicrobial potential and photodegradation efficiency which may be attributed to ROS generation as a result of synergism of Mn and Fe³⁴.

Yttrium-doped ZnO-NPs were utilized as antimicrobial agents against *B. subtilis*, *S. typhi* and *E. coli*. Pure ZnO-NPs showed excellent antimicrobial efficacy against *S. aureus* while ZnO-NPs doped with Yttrium showed excellent inhibition

for all the tested strains³⁵. Hence, Y-doped ZnO-NPs can serve as inexpensive and good inorganic antimicrobial agents. Similarly, Ag-doped ZnO-NPs and Ni doped ZnO-NPs were successfully utilized in wastewater treatment plants and as an antimicrobial agent against *P. aeruginosa* and *B. subtilis*, respectively^{36,37}. Zinc-doped CuO-NPs serves as an excellent antimicrobial nanomaterial due to its effective antibacterial activity against MDR bacteria. These NPs liberate intracellular ROS that plays an important role in killing bacteria. Hence, Zn doped CuO-NPs were synthesized by Wu and coworkers via sono-chemical method which were shown to exhibit strong antibacterial activity. They were able to kill 99.0% bacteria within 10 min under dark conditions apart from significantly hampering the bacterial growth in LB culture medium. The formulated Zn doped CuO-NPs exhibited nanopiercing on bacterial membrane which accelerates the leakage of cytoplasmic leakage. Hence, such multidimensional Zn doped CuO-NPs nanorods and exhibit distinct antibacterial activity as compared to undoped ZnO-NPs or undoped CuO-Ce-Fe doped zinc NPs^{38,39}.

Antimicrobial efficacy of doping TiO_2 -NPs

Introduction of dopants into the synthesized NPs leads to the development of versatile antimicrobial materials that are finding utility as packaging materials and in other biomedical applications. The photo activation property of the oxide component of titanium nanoparticles (TiO_2 -NPs) makes them highly effective in antimicrobial screening. Their biocidal action arises due to the modulation of charge (electron-hole) carriers at the interface of the external surface of the material which is needed for imparting durable capability. The dispersion of inorganic phase and organic-inorganic interfacial contact was optimally achieved for TiO_2 -NPs by several researchers⁴⁰⁻⁴². These NPs possess broad-spectrum antimicrobial efficacy against gram-negative and *Gram-positive* bacteria, and several fungi. Since, the doped TiO_2 -NPs nanoparticles exert a non-contact biocidal property and are environmental friendly, they do not release potentially toxic ions, a property required to prepare disinfectants^{43,44}.

Titanate nanowires film was prepared by Xu and co-workers on a Ti substrate by hydrothermal technique. AgNPs were used to dope the prepared

nanowire followed by the deposition of chitosan. It resulted in increased surface area and enhancement in the biocompatibility of titanium implants⁴⁵. Doping of these wires with AgNPs further elevates the antimicrobial potential. Cell viability tests further indicated the involvement of Ag⁺ for hindering the growth proliferation. Earlier, cerium doped TiO₂-NPs were investigated for their excellent antibacterial potential against *E. coli*⁴⁶. Moreover, TiO₂-NPs doped with iron and indium exhibited greater antibacterial activities against *E. coli* and *S. aureus* in contrast to their naïve counterparts⁴⁷. Additionally, TiO₂-NPs and silica nanoparticle (TiO₂@SiO₂) were modified by AgNPs and characterized by SEM and EDAX. The result on antibacterial activities showed higher inhibition efficiency against *P. aeruginosa* bacteria and Trichophyton fungi⁴⁸. Similarly, pure TiO₂ and Ag-doped TiO₂-NPs were assessed for their antibacterial properties against *P. aeruginosa*, *E. coli* and *S. aureus* under visible-light irradiation⁴⁹. The viability of the attempted microorganisms was hampered by these NPs. Similarly, the disinfection efficiency of Ag-TiO₂-SiO₂ nanomaterials were determined under solar irradiations, in dark condition, UV-A and UV-C against *E. coli*. SiO₂ mixed with TiO₂ (Si to Ti = 10:90) increased the specific surface area of the obtained photocatalyst as compared to commercial TiO₂. Ag-TiO₂-SiO₂ nanomaterials exhibited higher disinfection efficiency than TiO₂-SiO₂ since both AgNPs and ions showed strong antimicrobial potential⁵⁰. The bactericidal effect of Ag-TiO₂-SiO₂ was improved under light in contrast to dark conditions. Moreover, the superior synergistic effect of Ag-TiO₂-SiO₂ was obtained under both solar light and UV-A.

Incorporation of Ag-doped TiO₂-NPs into natural rubber latex foam (NRLF) enhanced its antimicrobial potential under visible light⁵¹. Modified NRLF showed greater antibacterial activity against *S. aureus*, *E. coli* and *S. epidermidis* under visible light conditions. The spectrophotometric measurements confirmed the inhibition of bacterial growth by the modified NRLF. Therefore, it can be suggested that Ag-doped TiO₂-NPs modified NRLF can be exploited as a potential antimicrobial agent for making antibacterial natural rubber latex

foam materials. The antibacterial properties of N₂ doped TiO₂-NPs as sandwich films embedding Ag in between the two layers was investigated by Wong and co-workers. The antibacterial potential of these thin films was improved significantly in both dark and visible light, and could efficiently remove *S. pyogenes*, *A. baumannii*, *S. aureus* and *E. coli*⁵².

CONCLUSION

Doped NPs have gained significant attention in obtaining successful antimicrobial systems in the recent past since they prevent the aggregation of NPs and allow them to disperse in aqueous environments or other hydrophilic media. Doping modification is one of the most effective methods to regulate and control the interaction of NPs and bacteria. Hence, doped NPs are increasingly used to target bacteria as an alternative to antibiotics and have shown their utility in treating bacterial infections. Examples include the utilization of doped NPs in antibacterial coatings for implantable devices and medicinal materials to prevent infection and promote wound healing, in antibiotic delivery systems to treat disease, in bacterial detection systems to generate microbial diagnostics, and in antibacterial vaccines to control bacterial infections. The antibacterial mechanisms of doped NPs are poorly understood, but the currently accepted mechanisms include oxidative stress induction, metal ion release and non-oxidative mechanisms. The multiple simultaneous mechanisms of action against microbes would require multiple simultaneous gene mutations in the same bacterial cell for antibacterial resistance to develop; therefore, it is difficult for bacterial cells to become resistant to doped National Pension System (NPs).

ACKNOWLEDGEMENT

The authors gratefully acknowledge the research facilities provided by Center of Excellence in Genomic Medicine Research, King Abdulaziz University, Jeddah, Saudi Arabia.

Conflicts of interest

The authors state no conflict of interest.

REFERENCES

1. Piktel, E.; Niemirowicz, K.; Watek, M.; Wollny, T.; Deptula, P.; Bucki, R. *J. Nanobiotechnol.*, **2016**, *14*, 39-45.
2. Ansari, S.A.; Satar, R.; Panda, D.S.; Zaidi, S.K.; Chibber, S.; Khan, M.J.; Khan, T.A.; Jafri, M.A.; Alqahtani, M.H. *Iran. J. Biotechnol.*, **2014**, *12*, 1-7.

3. Thakur, R.S.; Agarwal, R. *Curr. Drug Ther.*, **2015**, *10*, 20-34.
4. Yin, J.; Deng, B. *J. Memb. Sc.*, **2015**, *479*, 256-275.
5. Zhang, X.; Wang, W.; Zhang, Y.; Zeng, T.; Jia, C.; Chang, L. *Coll. Surf. B Bioint.*, **2018**, *161*, 433-441.
6. Ansari, S.A.; Husain, Q. *Biotechnol. Adv.*, **2012**, *30*, 512-523.
7. Nasr, N.F. *Int. J. Curr. Microbiol. App. Sci.*, **2015**, *4*, 846-853.
8. Abraham, A.M.; Kannangai, R.; Sridharan, G. *Ind. J. Med. Microbiol.*, **2008**, *26*, 297-301.
9. Pelgrift, R.Y.; Friedman, A. *J. Adv. Drug Deliv. Rev.*, **2013**, *65*, 1803-1815.
10. Singh, R.; Smitha, M.S.; Singh, S.P. *J. Nanosci. Nanotechnol.*, **2014**, *14*, 4745-4756.
11. Khan, S.A.; Noreen, F.; Kanwal, S.; Iqbal, A.; Hussain, G. *Mater. Sci. Eng. C Mater. Biol. Appl.*, **2018**, *82*, 46-59.
12. Jiang, J.; Pi, J.; Cai, J. *Bioinorg. Chem. Appl.*, **2018**, *2018*, Article ID 1062562, 18 pages.
13. Shah, S.N.A.; Shah, Z.; Hussain, M.; Khan, M. *Bioinorg. Chem. Appl.*, **2017**, *2017*, Article ID 410735, 12 pages.
14. Koshkin, V.M.; Slezov, V.V. *Tech. Phys. Lett.*, **2004**, *30*, 367-369.
15. Kwon, S.G.; Chattopadhyay, S.; Koo, B.; Claro, P.C.S.; Shibata, T.; Requejo, F.G.; Giovanetti, L.J.; Liu, Y.; Johnson, C.; Prakapenka, V.; Lee, B.; Shevchenko, E. V. *Nano Lett.*, **2016**, *16*, 3738-3747.
16. Saptarshi, S.R.; Duschl, A.; Lopata, A.L. *J. Nanobiotechnol.*, **2013**, *11*, 26-32.
17. Kawanishi, M.; Ogo, S.; Ikemoto, M.; Totsuka, Y.; Ishino, K.; Wakabayashi, K.; Yagi, T. *J. Toxicol. Sci.*, **2013**, *38*, 503-511.
18. Manke, A.; Wang, L.; Rojanasaku, Y. *Biomed. Res. Int.*, **2013**, *2013*, Article ID 942916, 15 pages.
19. Reddy, K.M.; Feris, K.; Bell, J.; Wingett, D.G.; Hanley, C.; Punnoosea, A. *Appl. Phys. Lett.*, **2007**, *90*, 2139021-2139023.
20. Jones, N.; Ray, B.; Ranjit, K.T.; Manna, A.C. *FEMS Microbiol. Lett.*, **2008**, *279*, 71-76.
21. Liu, Y.; He, L.; Mustapha, A.; Li, H.; Hu, Z.Q.; Lin, M. *J. Appl. Microbiol.*, **2009**, *107*, 1193-1201.
22. Sood, S.; Sharma, N. *Adv. Sci. Eng. Med.*, **2016**, *8*, 468-476.
23. Samavati, A.; Ismail, A.F.; Nur, H.; Othaman, Z.; Mustafa, M.K. *Chin. Phy.*, **2016**, *25*, 46-53.
24. Hameed, A.S.H.; Karthikeyan, C.; Ahamed, A.P.; Thajuddin, N.; Alharbi, N.S.A.; Alharbi, S.A.; Ravi, G. *Sci. Rep.*, **2016**, *6*, 24312-24323.
25. Rana, S.B., Singh, R. P. P. *J. Mater. Sci. Mater. Electron.*, **2016**, *27*, 9346-9355.
26. Podporska-Carroll, J.; Myles, A.; Quilty, B.; McCormack, D.E.; Fagan, R.; Hinder, S.J.; Dionysiou, D.D.; Pillai, S.C. *J. Haz. Mat.*, **2017**, *324*, 39-47.
27. Guo, B.L., Han, P.; Guo, L.C.; Cao, Y.Q.; Li, A.D.; Kong, J.Z.; Zhai, H.F.; Wu, D. *Nano. Res. Lett.*, **2015**, *10*, 336-346.
28. Ali, I.M.; Ibrahim, I.M.; Ahmed, E.F.; Abbas, Q.A. *Open J. Biophys.*, **2016**, *6*, 1-9.
29. Sharma, N.; Jandaik, S.; Kumar, S. *Anais da Acad. Brasil. de Cien.*, **2016**, *88*, 1689-1698.
30. Shoba, V.; Krishnapriya, K.; Boopathy, R.A.; Elanchezhiyan, C.; Selvisabhanayakam, D. *Int. J. Curr. Res.*, **2013**, *5*, 299-302.
31. Oves, M.; Arshad, M.; Khan, M.S.; Ahmed, A.S.; Azam, A.; Ismail, I.M.I. *J. Saudi Chem. Soc.*, **2015**, *19*, 581-588.
32. Vijayaprasath, G.; Murugan, R.; Palanisamy, S.; Prabhu, N.M.; Mahalingam, T.; Hayakawa, Y.; Ravi, G. *J. Mater. Sci. Mater. Electron.*, **2015**, *26*, 7564-7576.
33. Srinivasan, N.; Kannan, J.C.; Satheeskumar, S. *Int. J. Chem. Tech. Res.*, **2015**, *7*, 1708-1712.
34. Sharma, N.; Jandaik, S.; Kumar, S.; Chitkara, M.; Sandhu, I.S. *J. Exp. Nano.*, **2016**, *11*, 54-71.
35. Mote, V.D.; Purushotham, Y.; Shinde, R.S.; Salunke, S.D.; Dole, B.N. *Ceramica.*, **2015**, *61*, 457-461.
36. Mary, J.A.; Vijaya, J.J. *Int. J. Innov. Res. Sci. Eng. Technol.*, **2015**, *4*, 9-15.
37. Hosseini, S.M.; Sarsari, I.A.; Kameli, P.; Salamati, H. *J. All. Comp.*, **2015**, *640*, 408-415.
38. Shruti, S.; Vimala, R. *Int. J. Pure App. Biosci.*, **2015**, *3*, 186-190.
39. Wu R, Zhang H, Pan J, Zhu H, Ma Y, Cui W, Santos HA, Pan G. *Adv. Mater. Interf.*, **2016**, *3*, 472-480.
40. Kubacka, A, Serrano C, Ferrer M, Lunsdorf H, Bielecki P, Cerrada ML, Fernandez-Garcia M, Fernandez-Garcia M. High-performance dual-action polymer-TiO₂ nanocomposite films via melting processing. *Nano Lett.*, **2007**, *7*, 2529-2534.

41. Kubacka, A.; Ferrer, M.; Fernandez-Garcia, M. *Appl. Catal., B* **2012**, *121-122*, 230-248.
42. Llorens, A.; Lloret, E.; Picouet, P.A.; Trbjevich, R.; Fernandez, A. *Trends Food Sci. Technol.*, **2012**, *24*, 19-29.
43. Hamming, L.M.; Qiao, R.; Messersmith, P.B. *Compos. Sci. Technol.*, **2009**, *69*, 1880-1886.
44. Kubacka, A.; Ferrera, M.; Cerrada, M.L.; Serrano, C.; Sanchez-Chaves, M.; Fernandez-Garcia, M.; de Andres, A.; Jimenez, R.J.; Fernandez-Martin, F.; Fernandez-Garcia, M. *Appl. Catal., B* **2009**, *89*, 441-447.
45. Xu, Z.; Li, M.; Li, X.; Liu, X.; Ma, F.; Wu, S.; Yeung, K.W.K.; Han, Y.; Chu, P.K. *ACS Appl. Mater. Interf.*, **2016**, *8*, 16584-16594.
46. Ali, Z.; Raj, B.; Vishwas, M.; Athhar, M.A. *Int. J. Curr. Microbial. App. Sci.*, **2016**, *5*, 705-712.
47. Amabye, T.G.; Birara, A. *J. Med. Chem. Tox.*, **2016**, *1*, 1-7.
48. Govindhan, P.; Pragathiswaran, C. *J. Nano. Technol.*, **2016**, *2*, 173-175.
49. Gupta, K.; Singh, R.P.; Pandey, A.; Pandey, A. *Beilst. J. Nanotechnol.*, **2013**, *4*, 345-351.
50. Hoang, N.T.T.; Tran, A.T.K.; Suc, N.V.; Nguyen, T.V. *Mat. Sci.*, **2016**, *3*, 339-348.
51. Rathnayake, I.U.; Ismail, H.; de Silva, C.R.; Darsanasiri, N.D.; Bose, I. *Iran. Polym. J.*, **2015**, *24*, 1057-1068.
52. Wong, M.S.; Chen, C.W.; Hsieh, C.C.; Hung, S.C.; Sun, D.S.; Chang, H.H. *Sci. Rep.*, **2015**, *5*, 11978-11989.